

Fingerprinting Dark Energy II: weak lensing and galaxy clustering tests.

Domenico Sapone*

*Departamento de Física Teórica and Instituto de Física Teórica,
Universidad Autónoma de Madrid IFT-UAM/CSIC,
28049 Cantoblanco, Madrid, Spain*

Martin Kunz[†]

*Département de Physique Théorique, Université de Genève,
24 quai Ernest Ansermet, CH-1211 Genève 4, Switzerland
Institut d'Astrophysique Spatiale, Université Paris-Sud XI, Orsay 91405, France and
Astronomy Centre, University of Sussex, Falmer, Brighton BN1 9QH, UK*

Luca Amendola[‡]

*University of Heidelberg, Philosophenweg 16, 69120 Heidelberg, Germany and INAF/Rome
(Dated: October 30, 2018)*

The characterization of dark energy is a central task of cosmology. To go beyond a cosmological constant, we need to introduce at least an equation of state and a sound speed and consider observational tests that involve perturbations. If dark energy is not completely homogeneous on observable scales then the Poisson equation is modified and dark matter clustering is directly affected. One can then search for observational effects of dark energy clustering using dark matter as a probe. In this paper we exploit an analytical approximate solution of the perturbation equations in a general dark energy cosmology to analyze the performance of next-decade large scale surveys in constraining equation of state and sound speed. We find that tomographic weak lensing and galaxy redshift surveys can constrain the sound speed of the dark energy only if the latter is small, of the order of $c_s \lesssim 0.01$ (in units of c). For larger sound speeds the error grows to 100% and more. We conclude that large scale structure observations contain very little information about the perturbations in canonical scalar field models with a sound speed of unity. Nevertheless, they are able to detect the presence of “cold” dark energy, i.e. a dark energy with non-relativistic speed of sound.

PACS numbers: 98.80.-k; 95.36.+x

I. INTRODUCTION

Even though there is ample observational evidence that the expansion rate of the Universe is accelerating [1, 2], there is still no convincing theoretical model that can explain the observations. The simplest model in agreement with the data is the cosmological constant. However, it suffers from size and coincidence problems. In addition, it is likely that an earlier phase of accelerated expansion happened that was not due to a cosmological constant [3]. This period, inflation, is normally modeled as being due to a scalar field. The same basic mechanism can explain the dark energy, and is often called Quintessence in this context [4]. Scalar field dark energy is often employed to model a general equation of state $w(z)$, although one can also build a perfect fluid with exactly the same first order perturbations [5].

Over the last few years it has become clear that w alone is not sufficient to distinguish between different models explaining the dark energy, and that the perturbations induced by the dark energy constitute a complementary

probe [6–12]. The contribution of dark energy fluctuations to the perturbation dynamics is generally small and can be very difficult to measure. In a recent paper some of us derived theoretical approximations to the perturbations generated in scalar field dark energy models [13]. In this paper, we will use these expressions to investigate how two cosmological probes that will be of great importance in the future, weak lensing (WL) and the full galaxy power spectrum, can be used to measure the typical features that appear in such models, specifically the existence of a sound horizon. Exploiting the advantage of analytical approximations, we will try to isolate in some detail where the signal comes from.

Anticipating the conclusion, we will show that even a full sky, tomographic, deep redshift and imaging survey cannot constrain significantly the sound speed of the dark energy unless it is smaller than, roughly, $0.01c^1$. Small values of c_s are not compatible with a scalar field description with standard kinetic term and require extensions like k-essence [14] but are in general not forbidden: we will show that even with $c_s = 0.01$, dark energy, although “cold”, remains much less clustered than dark

*Electronic address: domenico.sapone@uam.es

[†]Electronic address: Martin.Kunz@unige.ch

[‡]Electronic address: L.Amendola@thphys.uni-heidelberg.de

¹ Here c denotes the speed of light, and in the rest of the paper we will use units so that $c = 1$.

matter and will not develop non-linearities by the present time. The special case of $c_s = 0$ has some additional attractive features, in that such models can cross $w = -1$ [5, 15] and can act as unified models of dark energy and dark matter [16] (but are also subject to the “dark degeneracy” [17]). For such extreme cases however dark energy becomes non linear along with dark matter and appropriate non-linear corrections are needed, especially for the weak lensing probe.

The sound speed of the dark energy could be measured also by other effects, like the Integrated Sachs-Wolfe (ISW) effect, either on the CMB or cross-correlated with large-scale structure. In [18] it has been shown that the CMB ISW tail can put a lower limit to c_s^2 , while [19] finds that $c_s \approx 0.01$ is actually favored by the WMAP 3-year data. The ISW is complementary to the probes we consider here since it is sensitive to perturbations on larger scales.

As in [13] we set the anisotropic stress of the dark energy to zero, which is appropriate for scalar field dark energy and in general for standard gravity models. In order to investigate more general cases, for example modifications of General Relativity, a non-zero anisotropic stress would have to be taken into account [10], but this is left for future work.

In detail, the paper is organized as follows. We begin by discussing the main results obtained in [13]. We then use these results to study the impact of the scalar field dark energy perturbations on the weak lensing signal and on probes of galaxy clustering, paying special attention to whether the presence of a sound horizon can be detected (by measuring the sound speed c_s^2). We also discuss which aspect of these probes are most sensitive to the perturbations.

We finally investigate constraints on the integrated deviation from the Poisson equation, which we call W , which may be useful to quantify the power of probes beyond the conventional, w -based Figure of Merit used by the dark energy task force [20].

II. SETTING THE SCENE

In this section we define our notation and present a short discussion of the perturbation equations and the approximate analytical solution of [13]. We refer the reader to that paper (and citations therein) for more details.

A. Definitions

In the following, the dots will refer to the derivatives with respect to the conformal time τ which is related to the universal time t by $dt = a(t) d\tau$. The physical

Hubble parameter that we will consider here is:

$$H^2 = \left(\frac{da}{adt} \right)^2 = H_0^2 [\Omega_{m,0} a^{-3} + (1 - \Omega_{m,0}) g(a)] \quad (1)$$

where $g(a) = \exp \left[-3 \int \frac{1+w(a)}{a} da \right]$ and the subscript 0 denotes the present epoch. This expression implies that we limit ourselves to a flat universe which is filled with matter (designated by a subscript m) and a general fluid with average pressure $p = w\rho$. In general the equation of state parameter w is a function of time, but we will take it to be constant later on.

We will consider linear perturbations about this spatially-flat background model, defined by the line element:

$$ds^2 = a^2 [-(1 + 2\psi) d\tau^2 + (1 - 2\phi) dx_i dx^i]. \quad (2)$$

As is apparent from the line element, we use the conformal Newtonian (longitudinal) gauge and retain only scalar perturbations. The perturbation equations for a dark energy fluid with sound speed c_s and parameter of state w are:

$$\delta' = -\frac{V}{Ha^2} \left(1 + \frac{9a^2 H^2 (c_s^2 - w)}{k^2} \right) - \frac{3}{a} (c_s^2 - w) \delta + 3(1 + w) \phi', \quad (3)$$

$$V' = -(1 - 3c_s^2) \frac{V}{a} + \frac{k^2 c_s^2}{Ha^2} \delta + (1 + w) \frac{k^2}{Ha^2} \psi \quad (4)$$

where $V = (1 + w)(ik_i v^i)$ is a measure of the velocity perturbation, δ is the density contrast, and the prime here means the derivative with respect to the scale factor a . We parameterize the pressure perturbation as:

$$\delta p = c_s^2 \rho \delta + \frac{3aH (c_s^2 - c_a^2)}{k^2} \rho V, \quad (5)$$

where $c_a^2 = w - \frac{\dot{w}}{3H(1+w)}$ is the adiabatic sound speed and c_s^2 is the sound speed in the rest-frame of the dark energy fluid. As already mentioned, we assume that the parameter of equation of state w stays constant so that $c_a^2 = w$.

We also assume a vanishing anisotropic stress $\sigma = 0$ as is the case for Quintessence and K-essence models, and therefore we have $\psi = \phi$. Finally, the gravitational potential can be found with the help of the Einstein equations,

$$k^2 \phi = -4\pi G a^2 \rho \left(\delta + \frac{3aH}{k^2} V \right). \quad (6)$$

B. Analytical solutions for dark energy perturbations

If the universe is perfectly matter dominated, then $k^2 \phi$ is a constant. In [13] we used this result to derive analytical solutions to the perturbation equations for dark energy in different limits:

- **scales larger than the sound horizon.** The modes larger than the sound horizon are found for $k \ll aH/c_s$. In this case, we neglect all terms containing the sound speed in Eq. (4) and then in Eq. (3), effectively setting $c_s^2 = 0$. Neglecting a decaying solution for which $V \propto 1/a$ we find:

$$\delta(a) = (1+w)\delta_{in} \left(\frac{a}{1-3w} + \frac{3H_0^2\Omega_{m,0}}{k^2} \right), \quad (7)$$

$$V(a) = -(1+w)H_0\sqrt{\Omega_{m,0}}\delta_{in}a^{1/2}. \quad (8)$$

- **Scales smaller than the sound horizon.** For modes smaller than the sound horizon, $k \gg aH/c_s$, we consider only the terms containing k^2 . We find that the density perturbations become constant and that the velocity perturbations decay:

$$\delta(a) = \frac{3}{2}(1+w)\frac{H_0^2\Omega_{m,0}}{c_s^2k^2}\delta_{in}, \quad (9)$$

$$V(a) = -\frac{9}{2}(1+w)(c_s^2-w)\frac{H_0^3\Omega_{m,0}^{3/2}}{\sqrt{a}c_s^2k^2}\delta_{in}. \quad (10)$$

In these equations, the factor δ_{in} sets the overall scale of the perturbations, chosen so that the matter perturbations are $\delta_m = \delta_{in}a$ on sub-horizon scales. In addition, the dark energy perturbations depend on their present density fraction (equal to $1 - \Omega_{m,0}$ since the universe is taken to be flat) but only through the combination $\Omega_{m,0}h^2$, the equation of state parameter w and the sound speed c_s^2 . They are a function of both scale k and scale factor a .

Let us quickly compare dark energy and dark matter fluctuations. For large scales the dominant term in Eq. (7) is the term containing k . Dark matter has a similar solution except that $w_{DM} = 0$; the ratio of the squares (i.e. the power spectrum ratio) for large scales then will be :

$$\left(\frac{\delta_{DE}}{\delta_m} \right)^2 = (1+w)^2 \leq \frac{1}{25} \quad (11)$$

if $w \leq -0.8$. However, for small scales (but still larger than c_s/aH), the first term in Eq. (7) dominates; in this case the ratio is:

$$\left(\frac{\delta_{DE}}{\delta_m} \right)^2 = \left(\frac{1+w}{1-3w} \right)^2 \leq \frac{1}{17^2} \simeq 0.0035. \quad (12)$$

The dark energy perturbations are thus always suppressed relative to the dark matter perturbations, even for a very low sound speed (note that the solution Eq. (7) was obtained assuming $c_s^2 = 0$).

For the forecasts of this paper, it is important to know whether we have to worry about non-linear effects: the non-linear clustering of dark energy models is still badly understood and may depend on the precise action of the model, and it is not clear what corrections we would

need to apply. Outside the sound horizon, the dark energy perturbation track those in the dark matter by the factors given above. These are roughly upper limits as $w = -0.8$ is at the upper limit of what is still allowed, and values of w closer to -1 will lead to smaller dark energy perturbations. If $c_s = 0.01$ the sound horizon at the present is of the order of $c_s(2/H_0) \approx 60 \text{ Mpc}/h$. On these scales dark matter fluctuations are still linear and therefore dark energy fluctuations are safely below the non-linearity threshold. On sub-sound-horizon scales, dark energy perturbations stop growing and become quickly negligible relative to the dark matter perturbations. If c_s is smaller than 0.001 then the dark energy will behave much like dark matter on the cluster scales and an appropriate non-linear correction would be needed, especially on the small scales probed by weak lensing (the small scale cut-off in the galaxy clustering safely excludes non linear scales). Therefore we do not extend our analysis to such small sound speeds; we include however for completeness the extreme case $c_s = 0$, for which we assume that we can apply the same non-linear correction as for the dark matter – whether this is acceptable may in general depend on the precise action of the field.

III. IMPACT OF THE SOUND SPEED ON GALAXY CLUSTERING AND WEAK LENSING

In this section we discuss the effect of dark energy clustering on the galaxy and weak lensing probes. We derive approximate analytical expressions that show how the relevant quantities change with the sound speed. This will help understanding qualitatively the numerical results of the next section.

A. The Q parameter

Matter domination was a necessary ingredient to derive the solutions given above. However, dark energy comes to dominate eventually, and then the potential starts to decay and the perturbations grow more slowly or start to decrease.

It is difficult to capture this behavior accurately. A way around this problem can be found by looking at the variable $Q(k, a)$ which we introduced in [12] to describe the change of the gravitational potential due to the dark energy perturbations. Q is defined through

$$k^2\phi = -4\pi G a^2 Q \rho_m \left(\delta_m + \frac{3aH}{k^2} V_m \right). \quad (13)$$

If the dark energy or modification of gravity does not contribute to the gravitational potential (for example if the dark energy is a cosmological constant) then $Q = 1$. Otherwise Q will deviate from unity, and in general it is a function of both scale and time.

Introducing the comoving density perturbation $\Delta \equiv \delta + 3aHV/k^2$, we can write

$$k^2\phi = -4\pi G a^2(\rho_m\Delta_m + \rho_{DE}\Delta_{DE}). \quad (14)$$

We neglect radiation in this paper as we are interested in observational tests at late times where it is subdominant. Then Q is defined as

$$Q - 1 = \frac{\rho_{DE}\Delta_{DE}}{\rho_m\Delta_m}. \quad (15)$$

Using simply the solution for the perturbations during matter domination, as discussed in the previous paragraph, we find that the resulting expression for Q is surprisingly accurate even at late times. The reason is that both fluids, dark energy and matter, respond similarly to the change in the expansion rate so that most of the deviations cancel. We find that the sub-soundhorizon expression below is accurate at the percent level, while on larger scales there are deviations of about 10 to 20% by today (depending on w). The latter can be corrected ‘‘by hand’’ in order to obtain a more precise formula, but the expressions are sufficiently accurate for our purposes and we keep them as they are.

As we have set the anisotropic stress to zero, the perturbations are fully described by Q . In [13] we provided the following explicit expression for the $Q(k, a)$ which captures the behavior for both limits (above and below the sound horizon):

$$Q(k, a) = 1 + \frac{1 - \Omega_{m,0}}{\Omega_{m,0}} \frac{(1+w)a^{-3w}}{1 - 3w + \frac{2}{3}\nu(a)^2}. \quad (16)$$

Here we used $\nu(a)^2 = k^2 c_s^2 a / (\Omega_{m,0} H_0^2)$ which we defined through $c_s k \equiv \nu a H$ so that ν counts how deep a mode is inside the sound horizon. We see that during matter domination (used in the first expression for ν) a k mode moves ever more deeply inside the sound horizon as a grows, which is of course no surprise.

From Eq. (15) we see that the deviation of Q from 1 depends on the ratio of the energy density of the dark matter and the dark energy, and on the relative amount of perturbations. The former scales as a^{-3w} for a constant w and the latter behaves as discussed in the last section. For $\Omega_{m,0} = 0.25$ and $w = -0.8$ we have that

$$Q - 1 \approx \frac{3}{17} a^{2.4} \simeq 0.18 a^{2.4} \quad (17)$$

on scales that are larger than the sound horizon, $\nu \approx 0$. This is not a negligible deviation today, but it decreases rapidly as we move into the past, as the dark energy becomes less important.² As a scale enters the sound horizon, $Q - 1$ grows with one power of the scale factor

slower (since δ_{DE} stops growing), suppressing the final deviation roughly by the ratio of horizon size to the scale of interest. In the observable range, $(k/H_0)^2 \approx 10^2 - 10^4$. Therefore if $c_s \approx 1$, $Q \rightarrow 1$ and the dependence on c_s is lost. This shows that Q is sensitive to c_s only for small values, $c_s^2 \lesssim 10^{-2}$.

We can characterize the dependence of Q on the main perturbation parameter c_s^2 by looking at its derivative, a key quantity for Fisher matrix forecasts:

$$\frac{\partial \log Q}{\partial \log c_s^2} = -\frac{x}{(1+x)} \frac{Q-1}{Q}. \quad (18)$$

where $x = \frac{2}{3}\nu(a)^2/(1-3w) \simeq 0.2\nu(a)^2$ (with the last expression being for $w = -0.8$). For the values we are interested here, this derivative has a peak just inside the sound horizon, the exact position is

$$k_{max} = \frac{H_0}{c_s} \sqrt{\frac{3}{2}\Omega_{m,0}(1-3w)(1+z)} \left[1 + \frac{1+w}{1-3w} \frac{1-\Omega_{m,0}}{\Omega_{m,0}} (1+z)^{3w} \right]^{1/4}. \quad (19)$$

Today the sound horizon is given by $c_s \approx H_0/k$. It lies in the observable range of k for sound speeds of the order of $c_s \approx 0.01 - 0.001$. We plot the derivative as the red curve in Fig. 2, there and from Eq. (18) we can see that the shape is basically proportional to $-x/(1+x)^2$. The derivative with respect to c_s^2 (instead of $\log c_s^2$) contains an additional factor of $1/c_s^2$ which means that it will be boosted by several orders of magnitude for small sound speeds.

We will later forecast how well the deviation of Q from 1 due to the dark energy perturbations can be measured by future cosmological surveys.

B. The growth rate and the γ parameter

In the Λ CDM model of cosmology, the dark matter perturbations on sub-horizon scales grow linearly with the scale factor a during matter domination. During radiation domination they grow logarithmically, and also at late times, when dark energy starts to dominate, their growth is suppressed. It is well known that in Λ CDM the growth factor can be expressed as:

$$G(a) \equiv \frac{\delta_m(a)}{\delta_m(a_0)} = \exp \left\{ \int_0^a \frac{\Omega_m(a')^\gamma}{a'} da' \right\} \quad (20)$$

where $\gamma \sim 0.545$ is called the growth index. There are two ways to influence the growth factor: firstly at background level, with a different Hubble expansion. Secondly at perturbation level: if dark energy clusters then the gravitational potential changes because of the Poisson equation, and this will also affect the growth rate of dark matter. All these effects can be included in the growth index γ and we therefore expect that γ is a function of w and c_s^2 (or equivalently of w and Q).

² For this reason, early dark energy models can have a much stronger impact [21].

According to [22], the growth index depends on dark energy perturbations (through Q) as

$$\gamma = \frac{3(1-w-A(Q))}{5-6w} \quad (21)$$

where

$$A(Q) = \frac{Q-1}{1-\Omega_m(a)}. \quad (22)$$

However, dark energy perturbations (hence Q) are difficult to measure at least if the dark energy has a very low sound speed. The growth index factor seems to be a more promising parameter and several experiments are planned to measure this quantity. Furthermore, we can invert Eq. (21) and ask the question: in the absence of anisotropic stress which Q is needed to generate a given γ ? Using Eqs. (21) and (22) we have:

$$Q-1 = [1-\Omega_m(a)] \left[1-w - \frac{1}{3}(5-6w)\gamma \right]. \quad (23)$$

The last equation is worth another look: let us assume we measure the growth index $\gamma = 6/11$ (the value usually associated to the cosmological constant) then Eq. (23) becomes:

$$Q-1 = \frac{1}{11}(1+w)[1-\Omega_m(a)]. \quad (24)$$

If we are dealing with the cosmological constant then we have the expected result of $Q-1 = 0$. However, if $w \neq -1$ then we can evaluate the corresponding value of Q ; for instance, if $w = -0.8$ then we have $Q-1 \sim 10^{-2}$, which is a positive number. However, this value is fairly big for dark energy perturbations, see [13]. Moreover, for non-phantom models the quantity $Q-1$ is always positive due to the relative increase of dark energy perturbations and the $(1+w)$ factor; let us remind the reader that if the anisotropic stress is set to zero then Q fully describes the evolution of dark energy perturbations; so, we can think to rephrase the sentence as: if $Q-1 > 0$ which γ can we reach? Setting Eq. (23) positive we have

$$\gamma < \frac{3(1-w)}{5-6w} \quad (25)$$

which sets a sort of upper bound to γ ; moreover, this is the limit we have if dark energy perturbations are set to zero (which can be seen directly from Eq. (21)).

In general we can say that if the anisotropic stress is zero then dark energy perturbations always decrease the value of the growth index. If we want to allow for perturbations in the dark energy sector while increasing at the same time the growth index then we need a non zero anisotropic contribution; this is the case for the DGP model (treated as an effective dark energy perturbations, see [10]) where $\gamma \sim 0.68$.

Let us also consider the derivative of $\log G$ with respect c_s^2 to gain an idea of how strongly the growth factor depends on sound speed, and thus on the characteristics of the dark energy perturbations:

$$\frac{\partial \log G(a_1)}{\partial \log c_s^2} = c_s^2 \int_{a_0}^{a_1} \frac{1}{a} \frac{\partial \gamma}{\partial c_s^2} \log \Omega_m(a) \Omega_m(a)^\gamma da. \quad (26)$$

We can see more clearly the dependence on the parameters by noting that the quantity $\log \Omega_m(a) \Omega_m(a)^\gamma$ can be approximated as $\Omega_m(a) - 1$ for Ω_m close to unity (we use however the exact expressions in the calculations below). Eq.(26) then reads:

$$\begin{aligned} \frac{\partial \log G(a_1)}{\partial \log c_s^2} &= \frac{3c_s^2}{5-6w} \int_{a_0}^{a_1} \frac{\partial Q}{\partial c_s^2} \frac{da}{a} \\ &= -\frac{3}{5-6w} \int_{a_0}^{a_1} \frac{Q-1}{1+ba} da \\ &= -\frac{3}{5-6w} \frac{1+w}{1-3w} \frac{1-\Omega_{m,0}}{\Omega_{m,0}} \times \\ &\quad \times b \int_{a_0}^{a_1} \frac{a^{-3w}}{(1+ba)^2} da \end{aligned} \quad (27)$$

where $b = x/a \approx 0.2\nu^2/a$ is a constant during matter domination (the value of x today). We first consider two different limits

- $b \gg 1$ (sub-sound horizon regime):

$$\begin{aligned} \frac{\partial \log G}{\partial \log c_s^2} &= -\frac{3}{5-6w} \frac{1+w}{1-3w} \frac{1-\Omega_{m,0}}{\Omega_{m,0}} \times \\ &\quad \times \frac{1}{b} \int_{a_0}^{a_1} a^{-3w-2} da = \\ &= \frac{3}{5-6w} \frac{Q-Q_0}{1+3w} \end{aligned} \quad (28)$$

- $b \ll 1$ (super-sound horizon regime):

$$\begin{aligned} \frac{\partial \log G}{\partial \log c_s^2} &= -\frac{3}{5-6w} \frac{1+w}{1-3w} \frac{1-\Omega_{m,0}}{\Omega_{m,0}} \times \\ &\quad \times b \int_{a_0}^{a_1} a^{-3w} da = \\ &= -\frac{3b}{5-6w} \frac{(Q-1)a - (Q_0-1)a_0}{1-3w} \end{aligned} \quad (29)$$

Both of these derivatives, like the one of Q discussed further above, have a strong dependence on the sound speed. As before, the peak location is near the sound horizon, and again the derivative with respect to c_s^2 adds an additional $1/c_s^2$ factor so that small sound speeds will lead to much larger values of the derivative.

The numerical factor (including the w dependence) is -0.22 and -0.09 for $w = -0.8$, respectively. We also notice that the first limit does not depend on $Q-1$ like the derivative Q , but on $Q-Q_0$ as it is an integral. The growth factor is thus not directly probing the deviation of Q from unity, but rather how Q evolves over time. This is similar in the second limit, except that we probe the evolution of $(Q-1)x$.

We can find a unified formula which accounts for both regimes:

$$\frac{\partial \log G}{\partial \log c_s^2} = -\frac{3}{5-6w} \frac{(Q-Q_0)[(Q-1)x - (Q_0-1)x_0]}{(1-3w)(Q-Q_0) - (1+3w)[(Q-1)x - (Q_0-1)x_0]} \quad (30)$$

where Q_0 and x_0 are evaluated at $a = a_0 = 1$.

The derivative is shown as the blue dashed line in Fig. 2. Just as the Q derivative, the G derivative peaks close to the sound horizon, but is smaller than the one of Q at this redshift. It grows however with growing redshift due to its integral nature, while the other derivatives decrease.

C. Shape of the dark matter power spectrum

In order to quantify the impact of the sound speed on the matter power spectrum we proceed in two ways: we first use the CAMB output [23] (which contains the full information on dark energy perturbations) and then we consider the analytic expression from Eisenstein & Hu [24] (which does not include dark energy perturbations, i.e. does not include c_s).

As anticipated, we find here that the impact of the derivative of the matter power spectrum with respect to the logarithm of sound speed on the final errors is only relevant if high values of c_s^2 are considered; for instance if $c_s^2 = 1$ then the errors on the sound speed increase by about 10 times when the analytic formula in Ref. [24] is considered instead of the CAMB output. By decreasing the sound speed, the results are less and less affected, and are completely unchanged when $c_s^2 = 10^{-5}$. The reason is that for low values of the sound speed other parameters, like the growth factor, start to be the dominant source of information on c_s^2 , see Fig. 7. Since for large c_s our results show that the sound speed is practically not measurable with the probes here considered, we disregard this difference between the analytical fit and the CAMB output and use the analytical fit whenever we find it convenient, in particular in estimating the weak lensing Fisher matrix.

In Fig. 1 we show the derivative of the logarithm of the matter power spectrum (from CAMB) with respect to the logarithm of sound speed. It is easy to understand this result: In Fig. 3 of [13] we showed that the power spectrum decreases by a few percent in a smooth step-like fashion at a scale just inside the sound horizon. Here we see the derivative of this transition. Just like the step, the peak of the derivative is situated a little bit inside the sound horizon, as is the case for the other contributions as well.

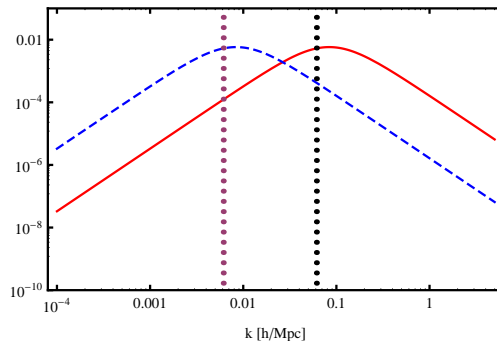


Figure 1: The figure shows the derivatives of the matter power spectrum with respect to $\log c_s^2$ for two different values of the sound speed: $c_s^2 = 10^{-2}$ and $c_s^2 = 10^{-4}$, red solid and blue dashed line, respectively. The vertical dotted lines give the scale of the sound horizon for two different sound speeds, $c_s^2 = 10^{-4}$ (left) and $c_s^2 = 10^{-2}$ (right).

D. Redshift space distortions

The velocity field of matter is directly sourced by the gradient of the ψ gravitational potential, and astronomers have been trying to measure it for a long time [25, 26]. More recently constraints on the velocity perturbations from redshift space distortions became an important probe for dark energy phenomenology, since their combination with weak lensing allows to disentangle the two potentials, which in turn allows to put limits on the anisotropic stress of the dark sector [12]. This is an important test for modifications of gravity [10]. Although there is no anisotropic stress in our scenario, we are nonetheless interested in how redshift space distortions are modified by the presence of dark energy perturbations.

The distortion induced by redshift can be expressed in linear theory by the β factor, related to the bias factor and the growth rate via:

$$\beta(z, k) = \frac{\Omega_m(z)^{\gamma(k,z)}}{b(z)}. \quad (31)$$

The derivative of the redshift distortion parameter with respect to the sound speed is:

$$\begin{aligned} & \frac{\partial \log(1 + \beta\mu^2)}{\partial \log c_s^2} \\ &= -\frac{3}{5-6w} \frac{\beta\mu^2}{1 + \beta\mu^2} \frac{x}{1+x} (Q-1). \end{aligned} \quad (32)$$

We see that the behavior versus c_s^2 is similar to the one

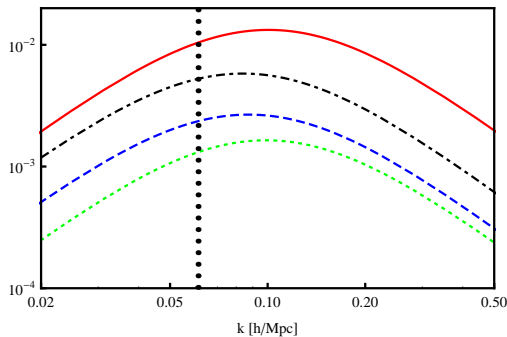


Figure 2: The figure shows the derivatives with respect to $\log c_s^2$ of the Q parameter Eq. (18) (red solid line), the growth factor Eq. (30) (blue dashed line), the redshift distortion parameter Eq. (32) (green dotted line) and the matter power spectrum $P_0(k)$ (black dot-dashed line). The derivatives are evaluated at a $z = 0.5$ except the one for $P_0(k)$ which is at $z = 0$; for all the derivatives the sound speed is $c_s^2 = 10^{-4}$. The vertical dotted line gives the scale of the sound horizon for $c_s^2 = 10^{-4}$ at $z = 0.5$.

for the Q derivative, so the same discussion applies. Once again, the effect is maximized for small c_s .

In Fig. 2 we compare the derivative of the redshift space distortion (green dotted line, averaged over μ) with those of the growth factor G and the Q variable. The β derivative is comparable to G at $z = 0$ but becomes more important at low redshifts and, as mentioned, is similar to the Q derivative in shape.

IV. OBSERVATIONAL CONSTRAINTS

A. Weak lensing

We want to investigate now the response of weak lensing (WL) to the dark energy parameters. We proceed with a Fisher matrix as in [12], to which we refer for the implementation details, the main difference here being that the parameter Q , which was general, now has an explicit form that describes how it changes as a function of scale and redshift. Since Q depends on w and c_s^2 , we can forecast the precision with which those parameters can be extracted. We can also try to trace where the constraints come from.

For WL experiments the important quantity is the lensing potential which is, using the metric Eq. (2):

$$\Phi = \phi + \psi. \quad (33)$$

For a vanishing anisotropic stress the WL potential becomes:

$$k^2 \Phi = -2Q \frac{3H_0^2 \Omega_{m,0}}{2a} \Delta_m. \quad (34)$$

In linear perturbation theory all k modes evolve independently, so that the dark matter density contrast is often

decomposed as:

$$\Delta_m(a, k) = aG(a, k) \Delta_m(k). \quad (35)$$

Here $\Delta_m(k) = \Delta_m(a=1, k)$ determines the matter power spectrum today, $P(k) = |\Delta_m(k)|^2$ and $G(a, k)$ is the growth factor, which depends here not only time but also on k since the dark energy perturbations in general introduce a scale dependence.

We can write Eq. (34) as:

$$k^2 \Phi = -3H(a)^2 a^3 Q(a, k) \Omega_m(a) G(a, k) \Delta_m(k) \quad (36)$$

where we used Eq. (35).

Hence, the lensing potential contains three conceptually different contributions from the dark energy perturbations:

- The direct contribution of the perturbations to the gravitational potential through the factor Q , see section III A.
- The impact of the dark energy perturbations on the growth rate of the dark matter perturbations, affecting the time dependence of Δ_m , through $G(a, k)$, cf section III B.
- A change in the shape of the matter power spectrum $P(k)$, corresponding to the dark energy induced k dependence of Δ_m , as discussed in section III C.

We consider a typical next-generation tomographic weak lensing survey characterized by the sky fraction $f_{sky} = 1/2$ and by the number of sources per arcmin², $d = 40$. We consider the range $10 < \ell < 10000$ and we extend our survey up to three different redshifts: $z_{max} = 2, 3, 4$. For the non linear correction we use the halo model by Smith et al. [27]. We choose as fiducial model $\Omega_{m,0} = 0.24$, $h = 0.7$, $\Omega_{DE} = 0.737$, $\Omega_K = 0$, $\Omega_b h^2 = 0.0223$, $\tau = 0.092$, $n_s = 0.96$, $w_0 = -0.8$, and several values for c_s^2 . The observationally borderline fiducial value of w_0 is chosen so as to maximize the impact on Q : values closer to -1 reduce the effect and therefore increase the errors on c_s .

We always plot the fully marginalized confidence ellipses (and quote fully marginalized errors) at 68%, which in 2D correspond to semi-axes of length 1.51 time the eigenvalues. In Fig. 3 we report the confidence region for w_0, c_s^2 for two different values of the sound speed and z_{max} . For high value of the sound speed ($c_s^2 = 1$) we find $\sigma(w_0) = 0.0171$ and the relative error for the sound speed is $\sigma(c_s^2)/c_s^2 = 2768$. As expected, WL is totally insensitive to the clustering properties of quintessence dark energy models when the sound speed is equal to 1. The presence of dark energy perturbations leaves a w and c_s^2 dependent signature in the evolution of the gravitational potentials through Δ_{DE}/Δ_m and, as already mentioned, the increase of the c_s^2 enhances the suppression of dark energy perturbations which brings $Q \rightarrow 1$.

WL		
c_s^2	σ_{w_0}	$\sigma_{c_s^2}/c_s^2$
10^{-5}	0.0257	0.49
10^{-4}	0.0232	2.48
10^{-3}	0.0211	8.34
10^{-2}	0.0192	44.58
10^{-1}	0.0183	282.6
1	0.0171	2768

Table I: Here are listed the errors for the equation of state parameter and the relative errors for the sound speed at $z_{max} = 3$.

Once we decrease the sound speed then dark energy perturbations are free to grow at smaller scales. As an example we show in the lower panel of Fig. 3, the confidence region for w_0, c_s^2 for $c_s^2 = 10^{-5}$, we find $\sigma(w_0) = 0.025$, $\sigma(c_s^2)/c_s^2 = 0.49$; in the last case the error on the measurement on the sound speed reduced to the 50% of the total signal.

In Tab. I we list the errors for w_0 and the relative errors of c_s^2 for six different values of the sound speed for a survey up to $z_{max} = 3$.

We should note here that the Fisher matrix approach breaks down for such large errors since it only considers the local curvature of the likelihood at the location of the fiducial model [28]. If we performed an actual analysis for data with $c_s^2 = 1$, we would find a lower limit near $c_s^2 = 10^{-5}$ since those models are measurably different from $c_s^2 = 1$ according to the lower panel of Figure 3, and the ellipse would be cut off there. On the other hand, there would not be any upper limit to c_s^2 since for all those cases the dark energy perturbations are not detected.

To explore more directly which term influences the most the weak lensing signal we assume that there are two different Q 's: one, Q_γ , which enters directly in the growth index expression (21) and the other, Q_Φ , which is the term that enters linearly in the expression of the gravitational potential (34). We concentrate here only on these terms since, as we mentioned previously, the changes on the matter power spectrum are negligible in the interesting range (i.e. for small sound speed).

- Q_γ only: Here we consider only the contribution from Q_γ setting effectively $Q_\Phi = 1$.
- Q_Φ only: Here we assume that dark energy perturbations enter only through Q_Φ , effectively setting the function $Q_\gamma = 1$ in Eq. (21).

We show the behavior of the errors in Fig. 4 as a function of the sound speed c_s^2 . We notice that the main contribution comes from Q_Φ . Keeping only this term leads to the same errors as the full expression. This is consistent with the discussion in sections III A and III B and the derivatives shown in Fig. 2 where we see that the growth factor is always less sensitive to the dark energy

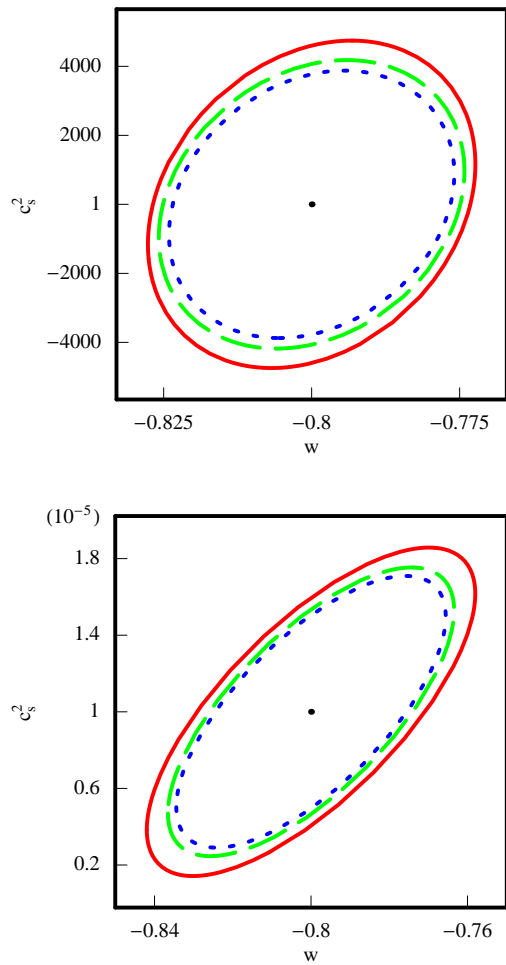


Figure 3: Confidence region at 68% for three different value of $z_{max} = 2, 3, 4$, blue dashed, green long-dashed and solid contour, respectively. The upper panel shows the confidence region when the sound speed is $c_s^2 = 1$; the bottom panel with the sound speed $c_s^2 = 10^{-5}$. The parameter equation of state is for both cases $w_0 = -0.8$.

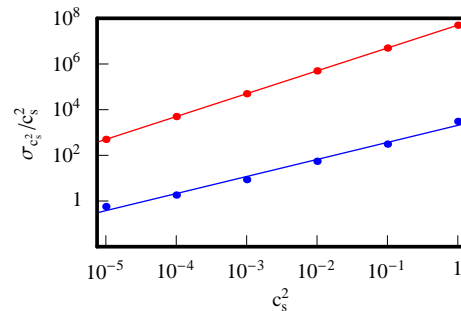


Figure 4: The figure shows the relative errors on the sound speed and their corresponding fits for our benchmark surveys; assuming only Q_γ in red and assuming only Q_Φ in blue.

perturbations than Q . As both enter in the same way in Eq. (36) the result is no surprise. At least for small sound speeds, gravitational lensing constrains directly the contribution of the dark energy perturbations to the metric, not their impact on the dark matter.

B. Galaxy power spectrum

We now explore a second probe of clustering, the galaxy power spectrum. Following [29] we write schematically the observed galaxy power spectrum as:

$$P_{obs}(z, k_r) = \frac{D_{Ar}^2(z)H(z)}{D_A^2(z)H_r(z)} G^2(z)b(z)^2 (1 + \beta\mu^2)^2 P_{0r}(k) + P_{shot}(z) \quad (37)$$

where the subscript r refers to the values assumed for the reference (or fiducial) cosmological model, i.e. the model at which we evaluate the Fisher matrix. Here P_{shot} is the shot noise due to discreteness in the survey, μ is the direction cosine within the survey, P_{0r} is the present spectrum for the fiducial cosmology, $G(z)$ is the linear growth factor of the matter perturbations, $b(z)$ is the bias factor (assumed scale independent) and D_A is the angular diameter distance.

The wavenumber k is also to be transformed between the fiducial cosmology and the general one ([29] and see also [30] and [31], for more details). To avoid non-linearity problems (both in the spectrum and in the bias), the Fisher matrix is calculated up to a limiting $k_{max}(z)$ at z : we choose values from $0.11h/\text{Mpc}$ for low- z bins to $0.3h/\text{Mpc}$ for the highest z -bins.

Here again the galaxy power spectrum is affected by the dark energy perturbations in three different direct ways:

- through the growth factor, see Eq. (21);
- through the redshift space distortions, see III D.
- through the present matter power spectrum P_{0r} , as discussed in III C.

We consider a photometric survey from $z = 0 - 2$ divided in equally spaced bins of width $\Delta z = 0.2$ as our benchmark survey; we assume an error on the measure of redshift of about $\delta z/z = 0.01$ and an area of 20000 deg^2 . These features are similar to those of proposed experiments like JDEM and Euclid, [32] and [33], respectively (see also DETF report [20]). Here too we also consider extended surveys to $z_{max} = 3$ and $z_{max} = 4$. Moreover, we assume an overall radial distribution $n(z) = z^2 \exp[-(z/z_0)^{1.5}]$ where $z_0 = z_{mean}/1.412$ and a $z_{mean} = 0.9$. The bias factor here is assumed to be only redshift dependent; we assume as fiducial bias $b(z) = \sqrt{1+z}$. In general, however, dark energy perturbations could lead to a scale dependence of the bias factor. Our fiducial model is exactly the same as for the WL survey considered in the previous section.

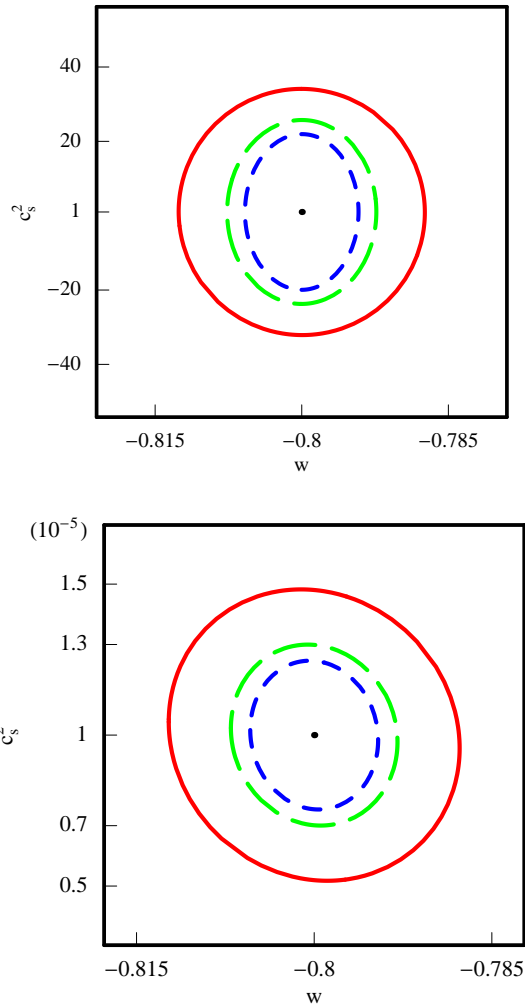


Figure 5: Confidence region at 68% for three different value of $z_{max} = 2, 3, 4$, blue dashed, green long-dashed and solid counter, respectively. The upper panel shows the confidence region when the sound speed is $c_s^2 = 1$; the bottom panel with the sound speed $c_s^2 = 10^{-5}$. The parameter equation of state is for both cases $w_0 = -0.8$.

In Fig. 5 we report the confidence region for w_0, c_s^2 for two different values of the sound speed and z_{max} . For high values of the sound speed ($c_s^2 = 1$) we find, for our benchmark survey: $\sigma(w_0) = 0.0088$, and $\sigma(c_s^2)/c_s^2 = 22.07$. Here again we find that galaxy power spectrum is not sensitive to the clustering properties of dark energy when the sound speed is of order unity. If we decrease the sound speed down to $c_s^2 = 10^{-5}$ then the errors are $\sigma(w_0) = 0.0091$, $\sigma(c_s^2)/c_s^2 = 0.32$.

In Tab. II we listed explicitly the errors for w_0 and the relative errors of c_s^2 for six different values of the sound speed for a benchmark survey up to $z_{max} = 2$.

We can ask again the question what part of the power spectrum is most sensitive to the dark energy perturbations, G , β or $P_0(k)$? In order to disentangle their relative contributions, we plot the corresponding diagonal Fisher

$P(k)$		
c_s^2	σ_{w_0}	$\sigma_{c_s^2}/c_s^2$
10^{-5}	0.009157	0.32
10^{-4}	0.009121	0.66
10^{-3}	0.009112	1.41
10^{-2}	0.009069	2.75
10^{-1}	0.008960	14.91
1	0.008825	22.07

Table II: Errors for the equation of state parameter and the relative errors for the sound speed for $z_{max} = 2$.

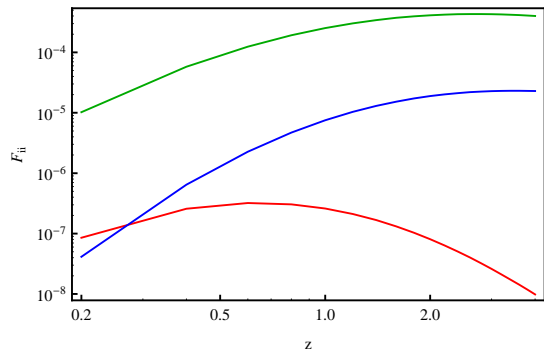


Figure 6: The figures shows the Fisher matrix element $G - G$, $\beta - \beta$, $P_0 - P_0$, solid blue, red and green lines, respectively. For $c_s^2 = 1$

matrix terms containing the sound speed as a function of redshift. The results are shown in Fig. 6 for $c_s^2 = 1$ and in Fig. 7 for $c_s^2 = 10^{-5}$. For large sound speed the shape of the dark matter power spectrum is formally the most sensitive, but not sufficiently to constrain the perturbations. In the more interesting case where the sound speed is lower and the perturbations can be detected, it is instead the growth factor that is the most sensitive.

In both cases the contribution from redshift space distortions to the overall constraints is sub-dominant except at redshifts below about $z = 0.3$ and for small c_s^2 , cf Figures 6 and 7. In the low-redshift region the growth factor is less sensitive as it is an integral from $z = 0$. To further clarify the importance of the redshift space distortions, we performed our analysis excluding the dependence of dark energy perturbations on the redshift distortion parameter. The result, given in Tab. III, shows that for small sound speeds the contribution from β is non-negligible when we compare it to Table II.

C. The scaling of the errors with c_s^2

In Fig. 8 the behavior in logarithmic scale of the sound speed errors $\sigma(c_s^2)/c_s^2$ are shown as a function of the sound speed itself. We notice that the errors appear to scale as a power law for both probes, over the range of sound

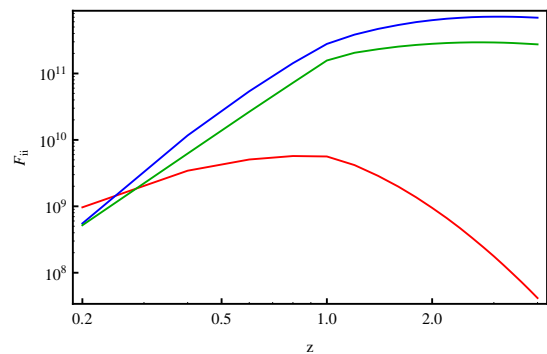


Figure 7: The upper panel shows $G - G$, $\beta - \beta$, $P_0 - P_0$, solid blue, red and green lines, respectively. For $c_s^2 = 10^{-5}$

$P(k)$			
	$z_{max} = 2$	$z_{max} = 3$	$z_{max} = 4$
c_s^2	$\sigma_{c_s^2}/c_s^2$	$\sigma_{c_s^2}/c_s^2$	$\sigma_{c_s^2}/c_s^2$
10^{-5}	0.67	0.48	0.41
1	22.48	15.32	12.69

Table III: Relative errors for c_s^2 for $P(k)$ for different z_{max} without redshift distortion.

speeds given. For the fiducial surveys we find

$$\frac{\sigma_{c_s^2}}{c_s^2} = 1830 (c_s^2)^{0.74} \quad (38)$$

for the weak lensing and

$$\frac{\sigma_{c_s^2}}{c_s^2} = 20.6 (c_s^2)^{0.387} \quad (39)$$

for the power spectrum.

D. Combined Fisher matrices and degeneracies.

We can also combine the two probes, the galaxy power spectrum and weak lensing, to improve the sensitivity to

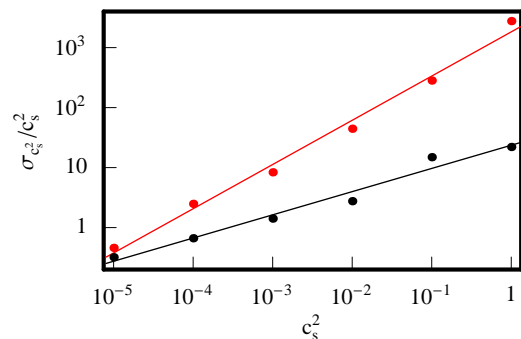


Figure 8: The figure shows the relative errors on the sound speed for two different experiments and their fits: WL in red and $P(k)$ in black, both for our benchmark survey.

	$\Omega_{m,0}h^2$	$\Omega_{b,0}h^2$	n_s	$\Omega_{m,0}$	w_0	c_s^2
$\Omega_{m,0}h^2$	1	-0.57	-0.55	-0.97	-0.57	-0.27
$\Omega_{b,0}h^2$	-0.57	1	0.23	0.64	0.49	0.22
n_s	-0.55	0.23	1	0.43	0.57	0.18
$\Omega_{m,0}$	-0.97	0.64	0.43	1	0.46	0.25
w_0	-0.57	0.49	0.57	0.46	1	0.30
c_s^2	-0.27	0.22	0.18	0.25	0.30	1

Table IV: Correlation matrix for galaxy power spectrum experiments and $c_s^2 = 10^{-5}$.

	$\Omega_{m,0}h^2$	$\Omega_{b,0}h^2$	n_s	$\Omega_{m,0}$	w_0	c_s^2
$\Omega_{m,0}h^2$	1	-0.25	0.88	-0.09	0.17	-0.01
$\Omega_{b,0}h^2$	-0.25	1	0.09	0.019	-0.39	-0.18
n_s	0.88	0.09	1	-0.32	0.22	-0.16
$\Omega_{m,0}$	-0.09	0.19	-0.32	1	-0.86	0.68
w_0	0.17	-0.39	0.22	-0.86	1	-0.23
c_s^2	-0.01	-0.18	-0.16	0.68	-0.23	1

Table V: Correlation matrix for WL experiments and $c_s^2 = 10^{-5}$.

the dark energy perturbations, cf. Tab. VIII. As expected the errors decrease by about 30% for low values of the sound speed and remain unaltered when the sound speed is close to unity.

We find that the sound speed does not suffer of any strong degeneracies with the other parameters considered in this work. We evaluated the dimensionless correlation matrix:

$$\text{Corr}_{ij} = \frac{C_{ij}}{\sqrt{C_{ii}C_{jj}}} \quad (40)$$

where C_{ij} is the inverse of the Fisher Matrix F_{ij} . For instance, for $c_s^2 = 10^{-5}$, we find for all parameters a correlation factor with c_s^2 of at most 0.3 for galaxy power spectrum experiments and at most 0.23 for WL experiments; however, for the latter case we find for $\Omega_{m,0} - c_s^2$ terms a correlation value of about 0.68. Increasing the sound speed the correlation terms decrease for galaxy power spectrum case and WL case; for the latter only the term $\Omega_b h^2 - c_s^2$ increases up to 0.78, for $c_s^2 = 1$.

E. An integrated measure of dark energy clustering

So far we have been studying the errors on the dark energy parameters w and c_s^2 . A subtly different question is whether we are able to detect dark energy perturbations or not – a question not about parameter constraints but about model probabilities [34]. It is not straightforward to use our constraints e.g. on the sound speed for this purpose, as it does not make sense to consider the speed of sound if there are no perturbations at all, i.e. a model without perturbations is not nested in the

quintessence model considered here. This is just another way to say that all quintessence models (except those for which $w = -1$, equivalent to a cosmological constant) necessarily have perturbations.

But from the errors on w and c_s^2 we can forecast the constraints on the amount of deviation of the Poisson equation from the expectation due to the dark matter and other known contributions, given by Q . A model without dark energy perturbations would then be characterized by $Q = 1$. However, Q is a function which evolves and additionally can have a scale dependence. It is then useful to define a compact way to express the deviation integrated over z and k . We define therefore the average quantity

$$W(\Omega_m, w, c_s^2) \equiv \frac{4\pi}{V_k \Delta z} \int |Q(k, z) - 1| dz k^2 dk \quad (41)$$

where Δz is the observed redshift range and $V_k = 4\pi k_{max}^2/3$ is the momentum volume. Finding a deviation of W from zero would signal some clustering of dark energy. We note that it is straightforward to focus on certain scales or epochs by introducing an appropriate weight function into the integral above.

In order to obtain constraints on W we need to marginalize the Fisher matrix over all parameters except $p_i = \{\Omega_m, w_0, c_s^2\}$ and then project it over the new parameter set $q_j = \{W, w_0, c_s^2\}$. Defining $J_{ij} = (\partial p_i / \partial q_j)_r$ we have

$$\sigma_{q_{ii}}^2 = (J_{ik} F_{kl} J_{li})^{-1}. \quad (42)$$

The errors on W for the $P(k)$ case are reported in Tab. VI and for WL in Tab. VII. Since the derivative of Q with respect the sound speed contains a term which goes like $1/c_s^2$, the dominating source of error on W comes from the errors on c_s^2 , as long as $c_s^2 \ll 1$. Therefore a quick estimate can be obtained by approximating

$$\frac{\sigma_W}{W} = \left| \frac{\partial \ln W}{\partial \ln c_s^2} \right| \frac{\sigma_{c_s^2}}{c_s^2} \approx \frac{\sigma_{c_s^2}}{c_s^2} \quad (43)$$

and we find that in the present case the relative errors on W are similar to those on c_s^2 . This supports the naive interpretation that we can only detect the perturbations if we can measure the sound speed, i.e. if the relative error on c_s^2 is less than unity.

However, we are now in a position where we can use model comparison techniques to decide whether $W \neq 0$ has been detected or not. Using the Savage-Dickey density ratio, we find that the relative model probability is given by the value of the normalized posterior (marginalized over all common parameters, i.e. all parameters except W) at $W = 0$, divided by the value of the normalized prior at the same place. To simplify the calculations, we choose a uniform prior in all variables except W , and for that variable a Gaussian pdf centered at $W = 0$ with a width (variance) Σ^2 . This then leads to a Bayes factor of

$$B_W = \sqrt{\frac{\bar{\sigma}^2}{\Sigma^2}} \exp \left\{ \frac{\bar{W}^2}{2\bar{\sigma}^2} \right\}. \quad (44)$$

$P(k)$		
c_s^2	σ_W/W	$\sigma_{c_s^2}/c_s^2$
10^{-5}	0.15	0.32
10^{-4}	0.42	0.66
10^{-3}	1.16	1.41
10^{-2}	2.53	2.79
10^{-1}	13.75	14.91
1	21.46	22.07

Table VI: Relative errors for W and the corresponding c_s^2 for $P(k)$.

Here \bar{W} is the value on which the posterior for W is centered, and $\bar{\sigma}^2$ the variance of W . Given the fiducial value W_{fid} and the Fisher matrix error σ_W^2 , which characterize the likelihood, we find for the posterior the shifted values (due to the prior, see e.g. the appendix of Ref. [35])

$$\bar{\sigma}^2 = \frac{\Sigma^2 \sigma_W^2}{\Sigma^2 + \sigma_W^2} \quad (45)$$

$$\bar{W} = \frac{\Sigma^2}{\Sigma^2 + \sigma_W^2} W_{\text{fid}}. \quad (46)$$

However, it is not obvious how we should choose the width of the prior, for a general model with unknown sound speed. One possibility is to use the most optimistic value, for which the model discrimination is maximal [36]. To find this value, we maximize B_W with respect to Σ , which leads to $\Sigma^2 = W_{\text{fid}}^2 - \sigma_W^2$. Using this prescription (valid only for $W_{\text{fid}} > \sigma_W$) we finally obtain

$$B_W = \sqrt{\frac{\sigma_W^2}{W_{\text{fid}}^2}} \exp \left\{ \frac{1}{2} \left(\frac{W_{\text{fid}}^2}{\sigma_W^2} - 1 \right) \right\}. \quad (47)$$

This formula depends only on the ratio W_{fid}/σ_W , and if we demand strong evidence in favor of the presence of perturbations, $\ln B > 5$, we find that we need $\sigma_W/W_{\text{fid}} \lesssim 0.27$, i.e. not quite a $4\text{-}\sigma$ detection. We remind the reader that this corresponds to the choice of prior that maximally favors the detection of perturbations, any other choice would need a stronger detection of W to reach the same Bayes factor.

Looking at tables VI, VII and VIII we can see that in our class of quintessence models and for the observations that we consider here, we can only hope to strongly favor the presence of dark energy perturbations if the sound speed is $c_s < 0.01$.

V. CONCLUSION

In this paper we extended the idea proposed in [13]. We investigated the effect of a generic modification of Poisson equation $Q(k, a)$ in the galaxy power spectrum and in the weak lensing convergence power spectrum induced solely by dark energy clustering. In other words,

WL		
c_s^2	σ_W/W	$\sigma_{c_s^2}/c_s^2$
10^{-5}	0.31	0.49
10^{-4}	2.13	2.48
10^{-3}	8.26	8.34
10^{-2}	44.39	44.58
10^{-1}	281.7	282.6
1	2766	2768

Table VII: Relative errors for W and the corresponding c_s^2 for WL.

$P(k)+WL$			
c_s^2	σ_{w_0}	$\sigma_{c_s^2}/c_s^2$	σ_W/W
10^{-5}	0.00639	0.15	0.11
10^{-4}	0.00581	0.41	0.36
10^{-3}	0.00547	0.87	1.02
10^{-2}	0.00531	2.48	2.39
10^{-1}	0.00528	14.79	13.14
1	0.00524	22.05	21.29

Table VIII: Errors for the equation of state parameter, the relative errors for the sound speed and the relative errors for the variable W combining WL and galaxy power spectrum probes.

we are using perturbations in the metric and in the dark matter to detect the tiny traces of dark energy perturbations.

We identified several effects: on the power spectrum growth, on its shape, and (for the galaxy clustering probe) on the redshift distortion. These effects are completely characterized by w and c_s^2 . We performed a Fisher matrix analysis of future large-scale surveys to forecast the errors on w and c_s^2 and therefore on $Q(k, a)$ or on its average version, W . As perhaps expected, we find that dark energy perturbations have a very small effect on dark matter clustering unless the sound speed is extremely small, $c_s \leq 0.01$. For $c_s \leq 0.01$, we find that W (that is, the average deviation for a standard Poisson equation) could be constrained to within 66% or better. Let us remind the reader that in order to boost the observable effect, we always assumed $w = -0.8$: for values closer to -1 the sensitivity to c_s^2 is further reduced; as a test we performed the calculation for $w = -0.9$ and $c_s^2 = 10^{-5}$ and we find $\sigma_{c_s^2}/c_s^2 = 2.6$ and $\sigma_{c_s^2}/c_s^2 = 1.09$ for WL and galaxy power spectrum experiments, respectively.

Such small sound speeds are not in contrast with the fundamental expectation of dark energy being much smoother than dark matter: even with $c_s \approx 0.01$, dark energy perturbations are more than one order of magnitude weaker than dark matter ones (at least for the class of models investigated here) and safely below non-linearity at the present time at all scales. Models of

“cold” dark energy with $c_s^2 = 0$ are interesting because they can cross the phantom divide [5] and contribute to the cluster masses [15]. Small c_s could be constructed for instance with scalar fields with non-standard kinetic energy terms. Here we showed that future large scale surveys have the potential to rule out or confirm this class of models. As an example we report here the absolute errors for the sound speed $c_s^2 = 0$: $\sigma_{c_s^2} = 0.344 \cdot 10^{-9}$ and $\sigma_{c_s^2} = 0.211 \cdot 10^{-7}$ for WL and galaxy power spectrum experiments respectively.

Acknowledgments

D. S. acknowledges support by the Spanish MICINN under the project AYA2009 – 13936 – C06 – 06 and the EU FP6 Marie Curie Research and Training Network ”UniverseNet” (MRTN – CT – 2006 – 035863). M.K. acknowledges support by the Swiss NSF.

-
- [1] A. G. Riess et al., *Astronomical J.* **116**, 1009 (1998).
 [2] S. Perlmutter et al., *Astrophys. J.* **517**, 565 (1999).
 [3] S. Ilic, M. Kunz, A.R. Liddle and J.A. Frieman, *Phys. Rev. D* **81**, 103502 (2010).
 [4] R. Caldwell, R. Dave, and P. J. Steinhardt, *Phys. Rev. Lett.* **80** 1582 (1998).
 [5] M. Kunz and D. Sapone, *Phys. Rev. D* **74**, 123503 (2006).
 [6] V.F. Mukhanov, H.A. Feldman and R.H. Brandenberger, *Phys. Rep.* **215**, 206 (1992).
 [7] V. Acquaviva, C. Baccigalupi and F. Perrotta, *Phys. Rev. D* **70**, 023515 (2004).
 [8] A. Lue, R. Scoccimarro and G.D. Starkmann, *Phys. Rev. D* **69**, 124015 (2004).
 [9] K. Koyama and R. Maartens, *JCAP* **0601**, 016 (2006).
 [10] M. Kunz and D. Sapone, *Phys. Rev. Lett.* **98**, 121301 (2007).
 [11] W. Hu and I. Sawicki, *Phys. Rev. D* **76**, 104043 (2007).
 [12] L. Amendola, M. Kunz and D. Sapone, *JCAP* **04**, 013 (2008).
 [13] D. Sapone and M. Kunz, *Phys. Rev D* **80**, 083519 (2009).
 [14] J. K. Erickson, J R. R. Caldwell, P. J. Steinhardt, C. Armendariz-Picon, & V. Mukhanov, *Phys. Rev. Lett.* **88**, 121301 (2002).
 [15] P. Creminelli, G. D’Amico, J. Norena, L. Senatore, & F. Vernizzi, *JCAP* **3** (2010), 27
 [16] C. Gao, M. Kunz, A.R. Liddle and D. Parkinson, *Phys. Rev. D* **81**, 043520 (2010).
 [17] M. Kunz, *Phys. Rev. D* **80** 123001 (2009).
 [18] J. Weller and A. M. Lewis, *Mon. Not. Roy. Astron. Soc.* **346** 987 (2003).
 [19] R. Bean and O. Dore *Phys. Rev. D* **69**, 083503 (2004).
 [20] A. Albrecht et al., Dark Energy Task Force report to the Astronomy and Astrophysics Advisory Committee, DETF <http://www.nsf.gov/mps/ast/detf.jsp>
 [21] R. de Putter, D. Huterer and E.V. Linder, *Phys. Rev. D* **81**, 103513 (2010).
 [22] E.V. Linder and R.N. Cahn, *Astropart. Phys.* **28**, 481 (2007).
 [23] A. Lewis, A. Challinor and A. Lasenby, *Astrophys. J.* **538**, 473 (2000).
 [24] D. Eisenstein and W. Hu, *Astrophys. J.* **511**, 5 (1999).
 [25] Courteau, S.A., Strauss, M. A., & Willick, J. A., Eds., 2000, ASP Conf. Ser. 201, Cosmic Flows (San Francisco: ASP)
 [26] P.G. Ferreira, R. Juszkiewicz, H.A. Feldman, M. Davis, A.H. Jaffe, *Astrophys. J.* **515** L1 (1999).
 [27] R. E. Smith et al., *MNRAS* **341**, 1311 (2003).
 [28] G. Ballesteros and J. Lesgourgues, arXiv:1004.5509 (2010).
 [29] H. J. Seo and D. J. Eisenstein, *Ap. J.* **598**, 720 (2003).
 [30] L. Amendola, C. Quercellini and E. Giallongo, *MNRAS* **357**, 429 (2005).
 [31] D. Sapone and L. Amendola, astro-ph/0709.2792.
 [32] A. Crofts et al. (2005), astro-ph/0507043.
 [33] A. Refregier et al. (2006); *Procs. of symposium “Astronomical Telescopes and Instrumentation”*; astro-ph/0610062.
 [34] P. Mukherjee, D. Parkinson, P.S. Corasaniti, A.R. Liddle and M. Kunz, *Mon. Not. Royal Astron. Soc.* **369**, 1725 (2006).
 [35] M. Kunz, R. Trotta and D. Parkinson, *Phys. Rev. D* **74**, 023503 (2006).
 [36] C. Gordon and R. Trotta, *Mon. Not. Roy. Astron. Soc.* **382**, 1859 (2007).